



Thermally responsive poly(*N*-isopropylacrylamide) monolayer on gold: synthesis, surface characterization, and protein interaction/adsorption studies

Eun Chul Cho, Yong Deuk Kim, Kilwon Cho*

Department of Chemical Engineering, Polymer Research Institute, Pohang University of Science and Technology, Pohang 790-784, South Korea

Received 26 November 2003; received in revised form 13 February 2004; accepted 24 February 2004

Abstract

This report describes a novel method for preparing a thermally responsive poly(*N*-isopropylacrylamide) (PNiPAM) monolayer on a gold surface, and demonstrates the function of this monolayer in aqueous media. Thiol (–SH) terminated PNiPAM was synthesized by UV polymerization followed by hydrolysis, and a monolayer of this polymer (2.84 ± 0.2 nm) was prepared on a gold substrate by simply dipping a pre-cleaned gold plate into an aqueous solution of the PNiPAM. Cyclic voltametry and atomic force microscopy studies showed that the gold surface was well covered by the PNiPAM chains, and X-ray photoelectron spectroscopic data showed that this monolayer was chemisorbed on the gold surface. Studies of the water contact angle, protein interaction, and protein adsorption on the PNiPAM monolayer demonstrated that this monolayer shows a temperature dependence of the interfacial properties in aqueous media.

© 2004 Elsevier Ltd. All rights reserved.

Keywords: Poly(*N*-isopropylacrylamide); Monolayer; Protein adhesion

1. Introduction

The fabrication of stimuli-sensitive surfaces (e.g. pH and temperature) has attracted considerable attention. These surfaces are typically prepared by grafting environmentally sensitive macromolecules onto a substrate, where the type of macromolecule and substrate are chosen depending on the intended use of the surface. A typical macromolecule used for this purpose is poly(*N*-isopropylacrylamide) (PNiPAM), which is known to show a lower critical solution temperature behavior at around 30 °C in aqueous media [1]. The phase transition of PNiPAM is accompanied not only by a rapid conformation change [2–6], but also by a change in interfacial free energy [7–11]. With above characteristics, this polymer has been used in drug delivery systems [12,13], tissue engineering [14,15], and in many other areas [16–22].

Numerous methods have been used to graft PNiPAM chains onto substrates [7–9,11,14,18,20,22–24]. These include chemical reaction between functionalized PNiPAM

and the substrate [7,22], and in situ polymerization of PNiPAM onto the substrates [8,9,11,14,18,20,23,24]. One system that has attracted particular attention is PNiPAM monolayers on a gold surface. This system has proved useful both in the study of the properties of PNiPAM using advanced techniques such as surface plasmon resonance (SPR) and quartz crystal analyzer (QCA), and in the preparation of thermally responsive gold nanoparticles. However, only a few studies are reported on this. Lopez et al. [11,20] and Jones et al. [18] prepared PNiPAM monolayers onto a self-assembled monolayer covered gold surface. Recently Shan et al. [25] prepared PNiPAM protected gold nanoparticles by various methods.

Here we report a novel method for preparing PNiPAM monolayers on a gold surface. Since the newly synthesized PNiPAM has a –SH group on the PNiPAM chain end, the PNiPAM monolayer can be directly formed by simply dipping the pre-cleaned gold substrate into an aqueous solution of PNiPAM. Therefore, the preparation method is less complex than previously reported methods. Here we describe in detail the methods for synthesizing the –SH terminated PNiPAM and for preparing PNiPAM monolayers on a gold surface. The surface of the resulting

* Corresponding author.

E-mail address: kwcho@postech.ac.kr (K. Cho).

monolayer was characterized to elucidate whether the PNiPAM chains well covered the gold surface. Finally, to assess the function of the PNiPAM monolayer in aqueous media, we measured the intermolecular forces between a protein and the PNiPAM monolayer by using atomic force microscopy (AFM), and conducted a protein adsorption study by QCA.

2. Experimental section

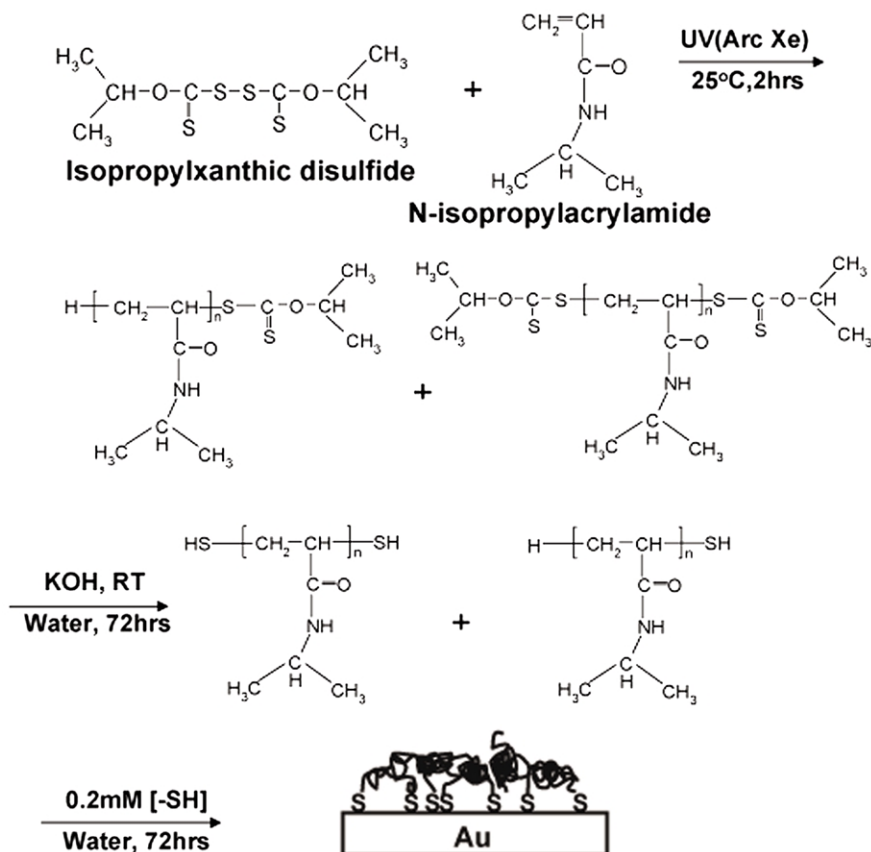
2.1. Synthesis of –SH terminated PNiPAM

Scheme 1 shows the synthesis of –SH terminated PNiPAM and the procedure for preparing the PNiPAM monolayer on the gold surface. The synthesis of –SH terminated PNiPAM was followed by the method of synthesizing other –SH terminated acrylic polymers [26]. Isopropylxanthic disulfide (Aldrich Chemical) that had been purified twice by recrystallization in acetone was used as the initiator and the chain transfer agent in this synthesis. *N*-isopropylacrylamide (Wako Pure Chemical Ltd., Japan) was purified twice by recrystallization in *n*-hexane.

The synthesis of –SH terminated PNiPAM required two steps. In the first step, the *N*-isopropylacrylamide monomer was photopolymerized with isopropylxanthic disulfide. The

monomer (20 g) and the initiator (0.12 g) were dissolved in tetrahydrofuran (20 g). The mixture was then degassed by freezing and thawing techniques, and then sealed off under vacuum. Then, the mixture was photopolymerized for 2 h with continuous stirring by using an Arc Xe lamp (440 W), and the resulting polymer was transferred into diethylether for purification. The viscosity of the mixtures starts to increase (visual inspection) when the reaction time reaches 60 min, but the mixture was further exposed to UV in order to obtain the high amount of PNiPAM (yield ~90%). There is a chance that the PNiPAM chain is chopped up by overexposing it to UV, but the rather narrow molecular weight distribution of this polymer in photoradical polymerization (PDI ~ 2.23, Table 1) indicates that the overexposure of the PNiPAM to UV does not damage seriously the PNiPAM chain. This purification was repeated two more times. The reaction product was further purified in water using dialysis. The final polymer was characterized by gel permeation chromatography (GPC), UV spectroscopy, and Fourier-Transform Infrared (FT-IR) spectroscopy.

In the second step, the isopropylxanthic sulfide group on the PNiPAM chain end was converted into the –SH group [27]. Two grams of photopolymerized PNiPAM was dissolved in 0.1 N KOH aqueous solution, and the resulting mixture was stirred for 3 days at room temperature. Then, the mixture was purified by dialysis, and finally the –SH



Scheme 1. Synthesis of the –SH functionalized PNiPAM and the preparation of PNiPAM monolayer on gold.

Table 1
Number average molecular weight of functionalized PNiPAM chain

Methods	GPC ^a		End group analysis ^b			
	Before hydrolysis		After hydrolysis		M_n (one end) ^c	M_n (two end) ^c
	M_n	PDI	M_n	PDI		
	20,900	2.23	19,900	2.19	14,100 ± 240	28,300 ± 480

^a In THF at 40 °C.

^b By UV spectroscopy.

^c M_n was calculated using UV spectroscopy by determining the concentration of the SC(=S)O moiety of the isopropylxanthic-terminated PNiPAM in ethanol on the assumption that the PNiPAM chain is terminated with an isopropylxanthic sulfide group on either one end or both ends. For further details, please see the text.

terminated PNiPAM was obtained by freeze-drying. The polymer product was characterized by GPC, UV spectroscopy, and FT-IR spectroscopy.

2.2. Preparation of the PNiPAM monolayer on gold

The PNiPAM monolayer on the gold surface was prepared as follows. A H₂ annealed gold (1000 Å) coated silicon wafer was sonicated with piranha solution (H₂SO₄/H₂O₂ = 7:3 by weight, this solution should be carefully handled) for 15 s and then washed with excess distilled water. The cleaned gold surface was further sonicated in ethanol for 1 h. A solution of PNiPAM in distilled water was prepared such that the –SH concentration was 0.1–0.2 mM. The clean gold surface was then dipped into the PNiPAM solution for 3 days at room temperature. After exhaustive washing with excess distilled water for removing the physisorbed PNiPAM layer, the PNiPAM monolayer was completely dried under vacuum.

2.3. Characterization of the PNiPAM monolayer

To check whether the PNiPAM chains covered the gold surface, we first measured the thickness of the PNiPAM monolayer by ellipsometry. In addition, cyclic voltametry was used to further assess whether the PNiPAM monolayer had achieved complete coverage. This method, which has been used to investigate the coverage of organic layers on metallic conducting surfaces [27], measures the current across the monolayer as a function of applied voltage. In this experiment, the PNiPAM monolayer was placed in an aqueous solution containing 1 mM K₄[Fe(CN)₆] and 1 M KCl, and the voltage (vs. a AgCl electrode)-current diagram (cyclic voltamogram) was recorded for the oxidation of Fe(CN)₆⁴⁻ to Fe(CN)₆³⁻. Pt was used as the counter electrode. The surface coverage of the PNiPAM monolayer was additionally assessed by comparing AFM (AutoProbe^R CR Research, Park Scientific Instrument) images of the bare gold surface with those of the gold surface covered with the PNiPAM monolayer.

X-ray photoelectron spectroscopy (XPS, VG Scientific, take-off angle 15°) was used to confirm the existence of the PNiPAM chains on the gold substrate and to check whether the PNiPAM chains were chemisorbed via Au–S bonds or simply physisorbed on the gold surface. Further, the equilibrium and dynamic contact angle of water on the PNiPAM monolayer were measured both at room temperature and at 40 °C to investigate whether this monolayer shows any temperature dependent change in the interfacial property with water.

2.4. Temperature-dependent interaction force between protein and PNiPAM monolayer and protein adsorption studies

To testify the function of the PNiPAM monolayer, we investigated the temperature dependent intermolecular force between the protein (bovine serum albumin, BSA) and the PNiPAM monolayer by AFM. BSA (Aldrich Chemical, molecular weight 67,000) was immobilized on the AFM tip, and the force–distance curve between the BSA-immobilized tip and the PNiPAM monolayer was measured while approaching and retracting the PNiPAM monolayer. The immobilization of proteins on the AFM tip was as follows. Firstly, the tip (Si₃N₄, spring constant of 0.05 N/m, radius ~307–50 nm) was exposed by oxygen plasma for 1 min to introduce the OH group on the AFM tip, and this was immediately transferred to the 10 mM γ -aminopropyltriethoxysilane toluene solution for 2 h at room temperature under the flow of Ar. Then the amine-terminated AFM tip was reacted with 10% v/v glutaraldehyde solution for 30 min at room temperature. Bovine Serum Albumin (BSA, Aldrich Chemical, molecular weight 67,000) was solubilized (1 mg/ml) in 10 mM phosphate buffer solution (pH 7.4), and the glutaraldehyde treated tip was dipped into the BSA solution for 40 min. After washing with phosphate buffer solution, the tip was stored in phosphate buffer solution at room temperature so that the BSA would maintain its natural conformation. We checked the existences of the BSA molecules on the AFM tip by a matrix-assisted laser desorption/ionization time of flight mass spectrometry (MALDI-TOF) analysis (data not shown).

In the force–distance curve (f–d curve) measurement between the PNiPAM monolayer and the BSA immobilized tip, 1 s was required to obtain the f–d curve during approaching and the retracting of the PNiPAM surface from the BSA immobilized tip. We applied the set force 1 nN and all the experiments were conducted in 10 mM phosphate buffer solution (pH 7.4). The adhesion force was measured at 25–34 °C in a custom-built temperature controlled liquid cell. For the reliability of our data, we used three different PNiPAM monolayer surfaces and the BSA immobilized tips.

We also used QCA (QCA917, SEIKO EG & G, Japan) to observe the temperature dependent protein adsorption behavior on the PNiPAM monolayer. The principle of

QCA is well described elsewhere [28]. A gold-coated (300 nm) AT-cut quartz electrode was cleaned and coated with a PNiPAM monolayer following the procedure described above for the treatment of the gold surface. The monolayer-covered electrode was equipped with a QCA holder, and the holder was dipped into 25 ml of phosphate buffer solution (pH 7.4, 10 mM). The holder was left in the phosphate buffer for at least 24 h in order to ensure that the resonant frequency was fully stabilized to within ± 3 Hz (we define this frequency as f_0). When the analyzer was equilibrated, 1 ml of BSA solution (5 mg/ml) was injected into the container equipped with the QCA holder. From this time, the BSA adsorption behavior was observed by in situ monitoring of the frequency of the electrode (f). Subtracting f_0 from f , we obtain the frequency change ($\Delta F = f - f_0$) with time of the PNiPAM monolayer electrode. The BSA adsorption behavior was examined at 22 and 37 °C (i.e. below and above the phase transition temperature of PNiPAM, respectively). The temperature was controlled within ± 0.1 °C using a circulation jacket. The frequency change was monitored every 1 s for 4 h.

3. Results and discussion

3.1. Characterization of the -SH terminated PNiPAM

Table 1 lists the number average molecular weight (M_n) and the polydispersity index (PDI) of the PNiPAM chain before and after hydrolysis, as determined by GPC. As can be seen in Scheme 1, it is expected that the introduction of SH group occurs by formation of ion pair between potassium ion and sulfide anion, which is the result of the cleavage of the S-C bond in the PNiPAM end. This ion pair was converted into the SH group by the hydrolysis. It is shown that M_n and the PDI do not change significantly after hydrolysis. We also determined M_n based on the UV spectrum of the isopropylxanthic terminated PNiPAM as follows. Since the $\pi-\pi^*$ transition of SC(=S)O absorbs in the UV region at about 279.4–279.2 nm (Fig. 1(a)), we measured the UV spectrum at various concentrations of isopropylxanthic sulfide and thereby generated the relationship between concentration of this species and UV absorbance in the target region. Then, we measured the absorbance of the isopropylxanthic sulfide terminated PNiPAM solution in the same region, and converted this absorbance to the concentration of this group. Since we knew the concentration of PNiPAM in the solution, we could determine the M_n of the isopropylxanthic terminated PNiPAM based on the assumption that the PNiPAM chains have either one or two such end groups. It should be noted that the linear relationship holds only when the UV absorbance is less than 1. Therefore, the concentration of both isopropylxanthic sulfide and the isopropylxanthic sulfide terminated PNiPAM should be prepared such that the measured absorbance is less than 1.

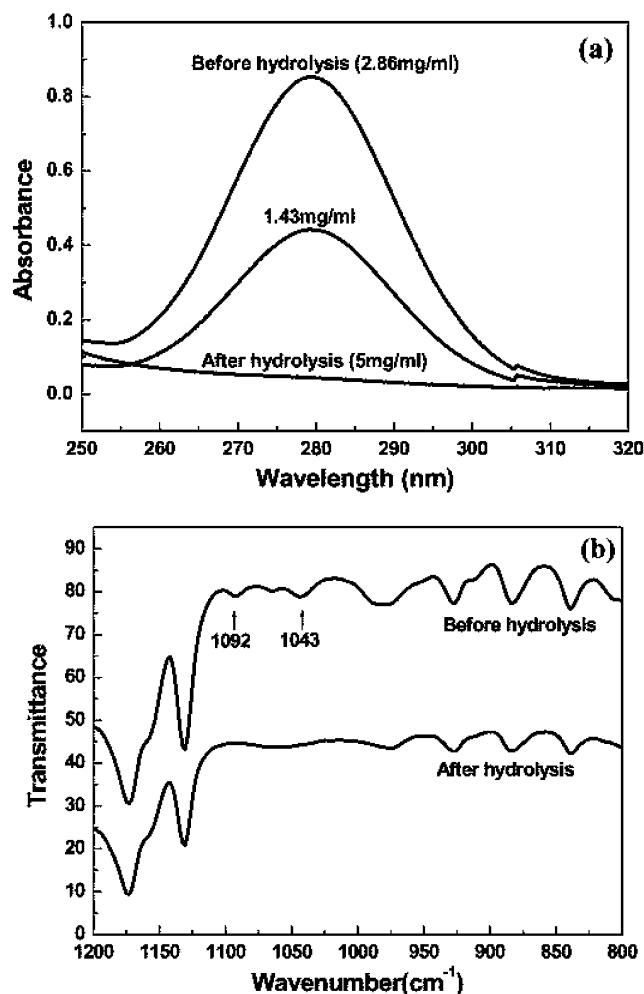


Fig. 1. (a) UV and (b) IR spectra before and after hydrolysis of the isopropylxanthic sulfide terminated PNiPAM. The concentration (Fig. 1(a)) is the polymer concentration in ethanol.

As can be seen in Scheme 1, isopropylxanthic disulfide is used as both an initiator and a chain transfer agent in this synthesis. As a result, the PNiPAM chains can have either one or two isopropylxanthic sulfide groups. For this reason, it is necessary to estimate how many thiol groups are attached on the PNiPAM chain. It should be noted that M_n determined by UV spectroscopy is not the same with that determined by GPC because M_n by GPC is affected by the elution solvent and the polymer standards used for calibration curve preparation in GPC analysis. Therefore, it is thought that the amount of end functional groups on the synthesized polymers should be estimated by comparing UV spectroscopy with NMR data. Unfortunately, we could not determine M_n by ^1H NMR because the proton peak in the PNiPAM chain was detected very broadly in the range of 1.1–2.3 ppm and we failed to discriminate the proton both in the isopropylxanthic sulfide and in the thiol groups. Therefore, we cannot exactly tell how many thiol groups are attached on the PNiPAM chain end. Alternatively, we tried to roughly estimate the number of thiol groups per PNiPAM chain by comparing M_n by UV with that by GPC within the

limitation stated above. The result shows that the PNiPAM chain has an average of 1.48 SC(=S)O groups per PNiPAM chain; that is, half of the PNiPAM molecules have one functional group, and the other half have two functional groups on both PNiPAM ends. Therefore, the chain conformation of the PNiPAM on the gold surface is expected to be the mixture of brush and bridge structures, as shown in Scheme 1.

Fig. 1(a) shows the UV spectra of the photopolymerized PNiPAM before and after hydrolysis in a 0.1 N KOH aqueous solution. Niwa et al. reported in Ref. [27] that the maximum absorbance of the π - π^* transition of SC(=S)O is at 282 nm. In our experiments, the maximum for this group was observed at 284.6 nm for isopropylxanthic disulfide and at 279.4–279.2 nm for isopropylxanthic sulfide terminated PNiPAM in ethanol. The maximum for this group was observed at 281 nm in water. This peak was not detected after the PNiPAM had been hydrolyzed in 0.1 N KOH solution. FT-IR spectra of the same systems (Fig. 1(b)) show peaks at 1043 and 1092 cm^{-1} before hydrolysis of PNiPAM but not after hydrolysis. By comparison with reference data [29], these peaks are attributed to the asymmetric stretch of the aliphatic ether (C–O–C) linkage in the isopropylxanthic sulfide group. Although the –SH group cannot be directly detected using UV and FT-IR spectroscopy, we infer from Fig. 1 that the isopropylxanthic sulfide group on the PNiPAM end is completely converted to the thiol group.

3.2. Surface analysis of the PNiPAM monolayer on a gold substrate

The thickness of the PNiPAM monolayer was determined by ellipsometry to be 2.84 ± 0.2 nm. This value is about 0.4 of the diameter of the PNiPAM chain (6.7 nm; this value was obtained assuming that the characteristic ratio of PNiPAM is similar to those of acrylic polymers, i.e. 8) [30]. This indicates that a pancake-type monolayer is formed on the gold surface. Since the PNiPAM chains have either one or two –SH groups, it is expected that the PNiPAM chains are spread on the gold surface more than the case when these have only one –SH group (Scheme 1).

Although the thickness of the PNiPAM monolayer is very small, the PNiPAM chains well cover the gold surface. Fig. 2 shows typical cyclic voltammograms for the clean gold substrate and for the PNiPAM monolayer on the gold substrate. In these voltammograms, an increase in electric current indicates increased oxidation of the electroactive species ($\text{K}_4[\text{Fe}(\text{CN})_6]$) on the surface, and a shift of the curve to higher voltage indicates that a higher voltage is required to oxidize the electroactive species. Thus, greater coverage of the gold surface with organic material is expected to manifest as a lower current and a shifting of the curve to higher voltage. The voltammogram for the clean gold surface (Fig. 2) shows a large oxidation reaction, and is similar to that reported by Niwa et al. [27]. In contrast, the CV curves for the PNiPAM–S–Au showed no oxidation

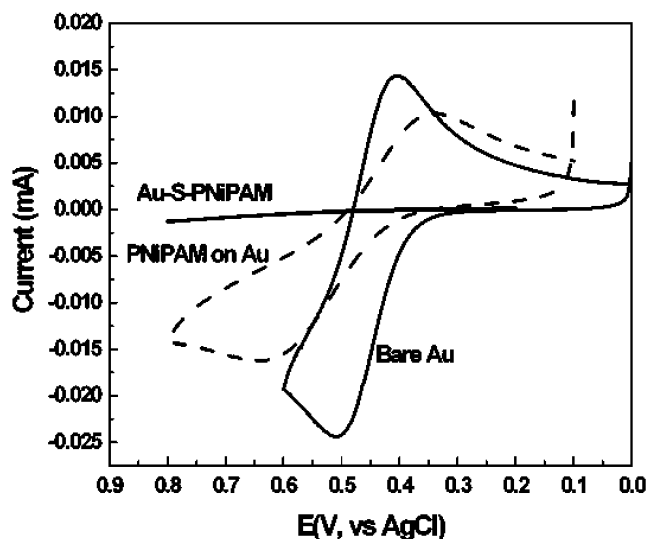


Fig. 2. Cyclic voltammograms for the cleaned gold surface and the PNiPAM monolayer on the gold surface.

reaction takes place at this surface, which indicates that contact of $\text{Fe}(\text{CN})_6^{4-}$ with the surface of the electrode was very restricted. For comparison, we also measured the CV voltammogram for a gold surface that had been dipped into an aqueous solution of unfunctionalized (without SH group) PNiPAM for 3 days. The unfunctionalized PNiPAM was synthesized by free radical polymerization using 2,2'-azobisisobutyronitrile as an initiator, and GPC results showed that M_n of this polymer was $\sim 16,000$ with PDI of 3.1. As can be seen in Fig. 2, the CV voltammogram for this surface indicates that oxidation does take place on this surface to a considerable extent. Based on these findings, we conclude that the unfunctionalized PNiPAM incompletely covers the gold surface, whereas the –SH terminated PNiPAM chains well cover the gold surface via Au-sulfide bond.

The surface coverage of the PNiPAM chains on the gold surface was additionally assessed by comparing AFM images of the PNiPAM covered gold surface (Fig. 3(b)) with those of the bare gold substrate (Fig. 3(a)). As can be seen in Fig. 3, the needle-like structure of the bare gold surface (rms roughness 2.95 nm) is smoothed out by the coverage of the PNiPAM chains (rms roughness 1.18 nm), consistent with the gold surface being well covered with PNiPAM chains.

To determine whether the PNiPAM layer is physically or chemically adsorbed onto the gold surface, we analyzed the PNiPAM monolayer using XPS. As can be seen in Fig. 4(a), the half-width in the C1s peak for the PNiPAM monolayer on the gold surface is broader than that for the clean gold surface; this is due to the C–N peak at 286.2 eV, [20,24]. The presence of the C=O peak at 287.8 eV provides clear evidence of the presence of PNiPAM on the gold surface. We also conducted the deconvolution of the C1s for the PNiPAM monolayer covered gold surface (inset in Fig. 4(a)). The ratio of C–H and C–C/C–N/C=O is

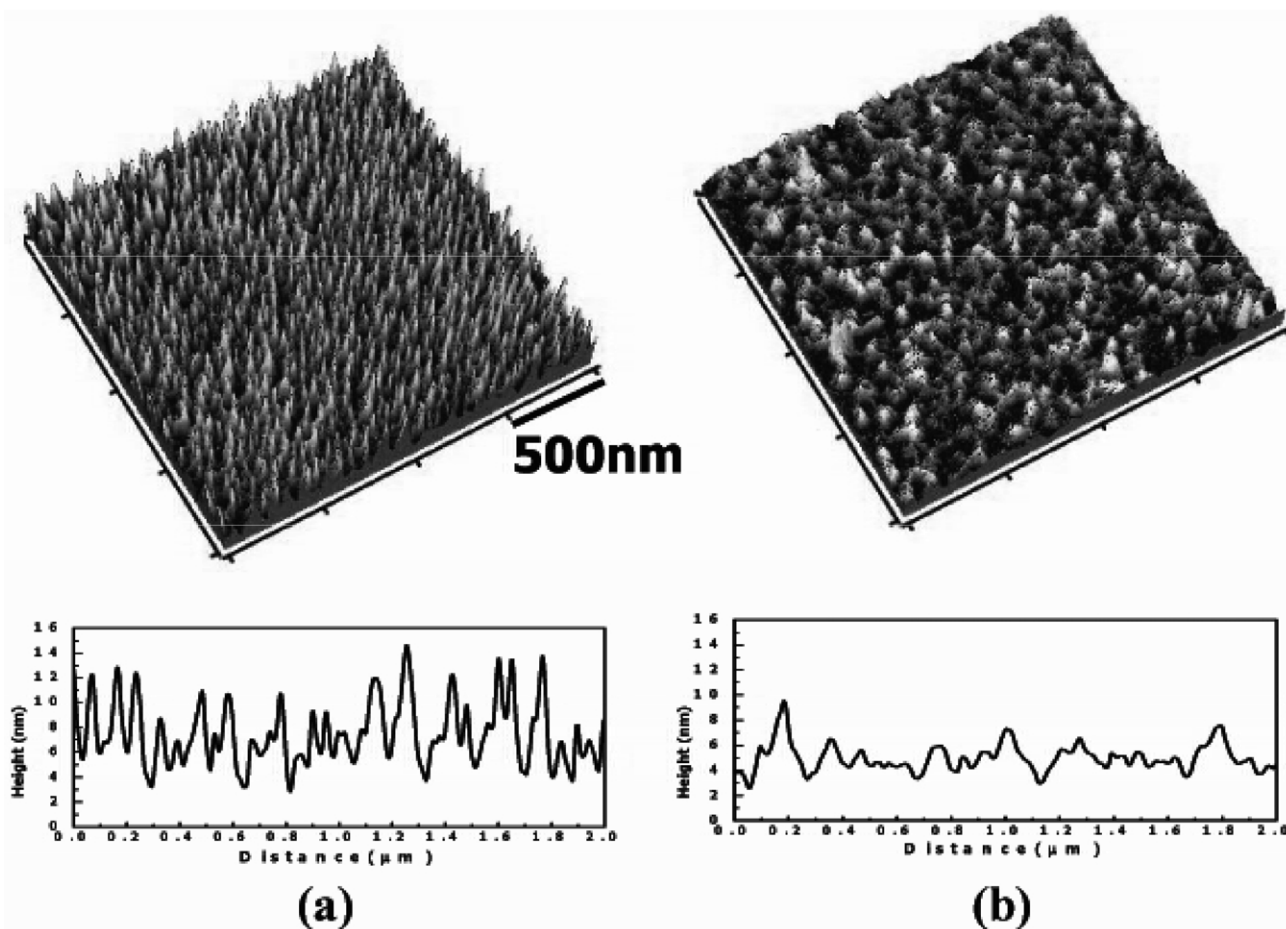


Fig. 3. AFM images (upper) and the roughness profiles (lower) for (a) the bare gold and (b) the PNiPAM monolayer on the gold surface.

69.3:13.8:16.9, and this result agrees with the theoretical value of 66.7:16.7:16.7 and with other reference [24].

In addition to the C1s spectra, the peaks at Au 4f_{7/2} (84.0 eV) and Au 4f_{5/2} (87.6 eV) observed for the bare gold surface (Fig. 4(b)) are split into two peaks for the case of PNiPAM–S–Au (84.0 and 84.5 eV for Au 4f_{7/2} and 87.6 and 88.1 eV for Au 4f_{5/2}, respectively), indicating that the PNiPAM chains are chemisorbed on the gold surface via Au–S bonds [31].

Measurements of the water contact angles on the PNiPAM monolayer (Table 2) provided additional evidence that the gold surface is well covered with PNiPAM chains. The water contact angle on the PNiPAM surface was found to be $62.2^\circ \pm 2.0^\circ$ at room temperature, which is very different from the value of $92^\circ \pm 1.6^\circ$ observed for the bare

gold surface. Comparison of the water contact angle on the PNiPAM surface at room temperature with that at 40 °C (Table 2) revealed a temperature dependence in the properties of the interface between the PNiPAM monolayer and water. Although the receding water contact angle changes little, both the equilibrium and the advancing water contact angles vary considerably on going from room temperature to 40 °C. This is in agreement with a previous report on the contact angle of the PNiPAM brush onto the self-assembled monolayer-covered gold surface [11]. However, different results have been reported for the temperature dependence of the dynamic water contact angles. Liang et al. [9] and Ista et al. [20] found that the advancing contact angle changed from $\sim 50^\circ$ to $70\text{--}80^\circ$ on going through the phase transition. In contrast, Schmitt et al. [10] and Kidoaki et al.

Table 2

Water contact angle on the PNiPAM monolayer

Gold (equilibrium)	PNiPAM monolayer on gold					
	Room temperature			40 °C		
	Equilibrium	Advancing	Receding	Equilibrium	Advancing	Receding
$92^\circ \pm 1.6^\circ$	62.2 ± 2.0	65.7 ± 4.3	30.5 ± 1.6	72 ± 1.4	79.9 ± 0.8	32.9 ± 2.8

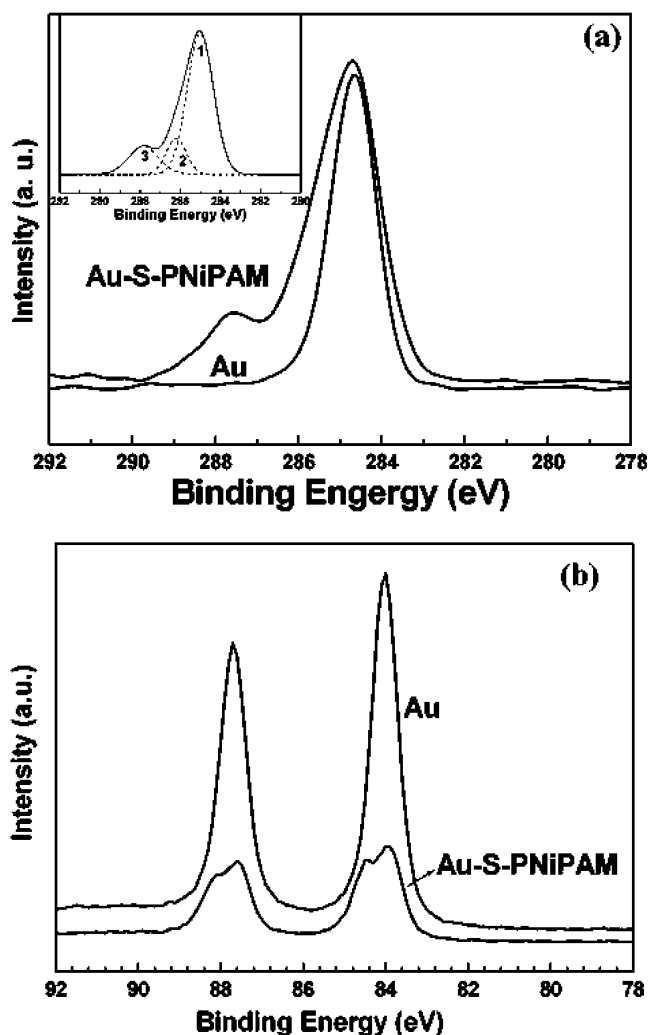


Fig. 4. XPS analysis of the bare gold surface and the PNiPAM monolayer on the gold surface. (a) C1s, (b) Au 4f. Inset in Fig. 4(a) shows the deconvolution of C1s for the PNiPAM monolayer on gold surface: 1, C1s for C–C and C–H; 2, for C–N; 3, for C=O. The spectra were calibrated with respect to the C–H peak at 285.0 eV.

[23] reported that the advancing angle was unaffected by the phase transition, whereas the receding angle changed from 18° to 30°. To date, no clear explanation has been given for these apparent discrepancies.

3.3. Temperature dependence of the intermolecular force between BSA and the PNiPAM monolayer

To determine whether the PNiPAM monolayer responds to temperature changes in the aqueous system, we used AFM to probe the intermolecular force between BSA and the PNiPAM monolayer in a phosphate buffer solution (pH 7.4) at temperatures in the range 25–34 °C. Fig. 5(a) shows the force–distance curves between the BSA-immobilized tip and the PNiPAM monolayer recorded at 25–34 °C. In this figure, the ‘zero’ distance is defined as the point at which there is no absolute measure of force for the distance between tip and surface. This does not mean the point that

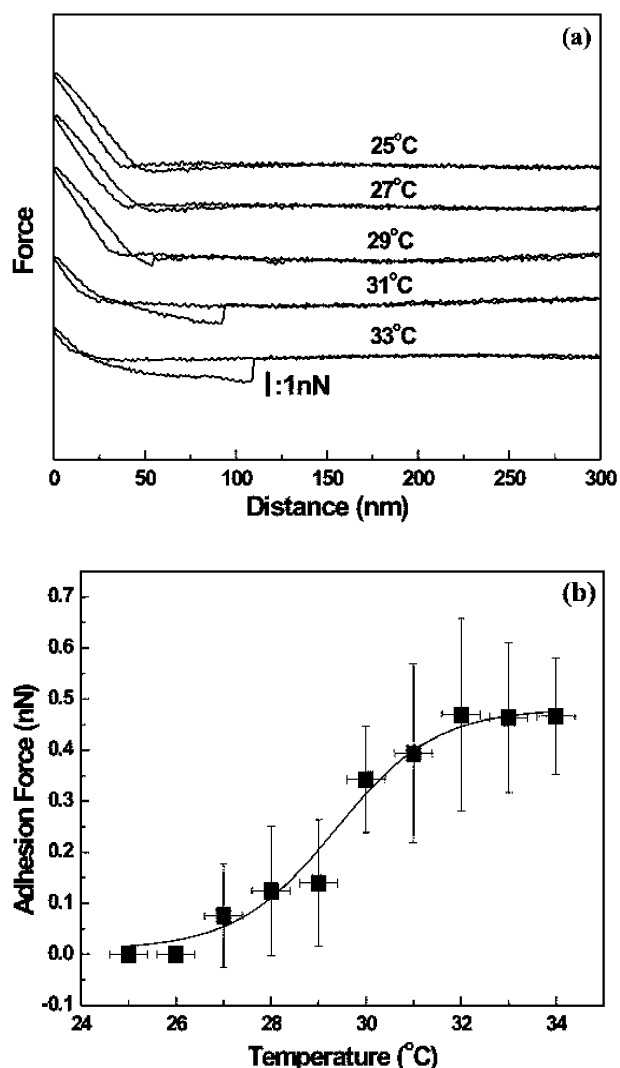


Fig. 5. (a) Force–distance curve for the BSA immobilized tip and the PNiPAM monolayer in the range 25–32 °C. (b) Temperature dependent maximum adhesion force between the BSA immobilized tip and the PNiPAM monolayer. The maximum adhesion force was obtained during retraction of the PNiPAM monolayer. All experiments were conducted in 10 mM phosphate buffer solution (pH 7.4).

the surface and the tip start to contact. At 25 °C, which is below the phase transition temperature of PNiPAM in water, there is no attractive force between the BSA-immobilized tip and the PNiPAM monolayer. However, as the temperature goes up an attractive force between the BSA immobilized tip and the PNiPAM surface starts to appear, and its magnitude increases as the temperature increases. Comparison of the adhesion force (maximum adhesion force during retraction of the PNiPAM monolayer) for temperatures in the range 25–34 °C (Fig. 5(b)) showed a change at around 29 °C (this was taken as an inflection point of guide line).

We compared the transition temperature of the PNiPAM monolayer from the AFM measurement (29 °C) with the transition temperature of PNiPAM in aqueous solution. The same SH-terminated PNiPAM as the PNiPAM used in

monolayer preparation was dissolved in distilled water and phosphate buffer (10 mM, pH 7.4) (3 wt%), respectively, and we carried out differential scanning calorimetry experiment (scanning rate of 3 °C/min) with these solutions. The transition peaks show 33.6 °C in distilled water and 32.9 °C in phosphate buffer, and these temperatures are higher than the transition temperature from AFM studies. The reason is not clear why the measured transition temperature is different between the grafted PNiPAM and the PNiPAM aqueous solution, but it is thought that the grafted PNiPAM chain molecules interact or behave differently from the PNiPAM chains in solution when they undergo transition temperatures.

The present observation of a change in the intermolecular forces between the BSA immobilized tip and the PNiPAM monolayer on passing through the phase transition temperature of PNiPAM is very similar to the behavior observed in our previous experiments on PNiPAM brushes ($M_n \sim 3100$, 4.4 nm in air) in an aqueous environment [32]. And we showed that the temperature dependent intermolecular force change results from the change in the interfacial properties of the PNiPAM grafted surface by showing that there is no temperature dependent change in the f - d curve between the BSA immobilized tip and CH_3 terminated and COOH terminated self-assembled monolayers ($\text{HS}(\text{CH}_2)_{11}\text{CH}_3$ and $\text{HS}(\text{CH}_2)_{11}\text{COOH}$) on gold surfaces. Kidoaki et al. [23] also measured the f - d curve for the interaction between an albumin-immobilized tip and the PNiPAM grafted surface. In contrast with our results, they showed that there is no adhesion force between the albumin tip and the PNiPAM surface for two temperatures, 25 and 40 °C. This result is different from our present study. They argued that the absence of adhesion at 25 and 40 °C is because of the hydrophilic nature of the albumin molecule. However, about half of the amino acids in the BSA molecule contain non-polar residues [33], and it is known that albumin molecules are the main carriers of fatty acids in the human body and have hydrophobic pockets within their structure [33,34]. The reason why our present data is different from theirs is not clear at this state, but it is thought that the different experimental condition (i.e. applied loading force to the tip and the frequency for the approach-retraction cycle (1 Hz in our experiment)) and the different tip immobilization procedure would result in the different results. However, from the result of most protein adsorption and cell adhesion studies [13,14,20–22], a certain magnitude of the adhesion force is expected above transition temperatures.

It has been suggested that the fully hydrated PNiPAM chains have abundant bound water molecules below the phase transition temperature of PNiPAM [35,36], and the PNiPAM chains themselves are very flexible [2–4]. When the protein molecules approach these fully hydrated PNiPAM chains, it is expected that, as is the case for poly(ethylene oxide) in water [37,38], the bound waters prevent intimate molecular contact between the two

surfaces, and steric repulsion of the flexible PNiPAM results in an intermolecular force of nearly zero. Above the phase transition temperature, less water molecules are bound to the PNiPAM chains and these chains take on a rather hydrophobic globular structure [2–4,35]. When protein molecules approach the PNiPAM surface, loosely bound water on the PNiPAM chain allows the some contacts between the PNiPAM chain and protein molecules, and a rather fixed globular PNiPAM does not show the steric repulsion against approaching protein molecules. Therefore, attraction force between BSA and the PNiPAM chain is expected above the phase transition temperature.

3.4. Temperature dependence of the adsorption of BSA onto the PNiPAM monolayer

We used QCA to determine the extent of protein adsorption on the PNiPAM monolayer (Fig. 6) below (22 °C) and above the phase transition temperature (37 °C). At 22 °C, $\Delta F (= f - f_0)$ changes to -10 ± 1.7 Hz 4 h after injecting the BSA solution. In contrast, the value of ΔF at 37 °C after 4 h is -54.5 ± 6.4 Hz, which is 5 times the value at 22 °C. Taking into consideration of previous reports that the amount of BSA adsorbed changes little over the temperature range used in the present work (22–37 °C) on the substrates with no temperature dependence [39], the difference in frequency change between 22 and 37 °C can be attributed to the change in the properties of the interface between the PNiPAM monolayer and the aqueous phase. The present QCA results agree well with those of other studies into protein adsorption on PNiPAM particles [21,22,40].

As can be seen in Figs. 5 and 6, the force–distance curve obtained using AFM and the protein adsorption data obtained by QCA show the same general trend and indicate that the properties of the PNiPAM monolayer are temperature dependent in the aqueous system. However, one noticeable

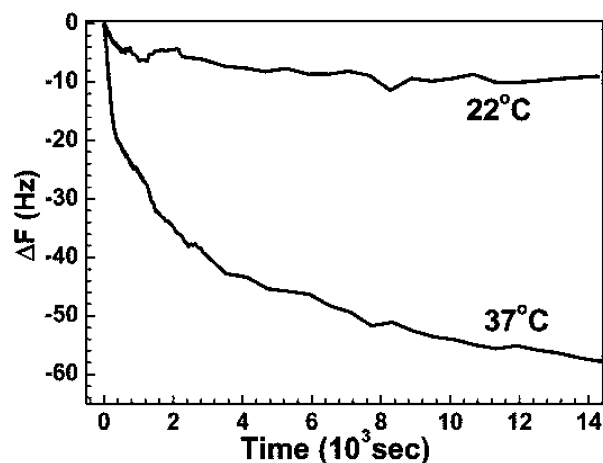


Fig. 6. BSA adsorption behavior on the PNiPAM monolayer at 22 and 37 °C. Experiment was conducted in 10 mM phosphate buffer solution (pH 7.4).

feature of Figs. 5 and 6 is the observation that a small amount of BSA is adsorbed on the PNiPAM monolayer at 22 °C (Fig. 6), despite AFM data indicating that the intermolecular force between the BSA-immobilized tip and the PNiPAM monolayer is nearly zero at 25 °C (Fig. 5). This can be qualitatively accounted for the effect of the short contact time (<1 s) between the protein and the PNiPAM chain used to measure the intermolecular force in the AFM experiments. In contrast to this brief contact, when the protein molecules are added to the aqueous phase in the QCA experiment they reside at the PNiPAM surfaces for much longer times. Hence, we speculate that the protein molecules, the waters bound to the PNiPAM chains, and the PNiPAM chains themselves might have sufficient time to change their structures so as to minimize the interfacial free energy at the PNiPAM/BSA interface. This conjectured behavior is similar to the common phenomenon whereby proteins and macromolecules undergo structural changes after adsorption onto a substrate to states that are more energetically favorable in the interfacial environment [41]. Therefore, the different results between the adsorption data obtained by QCA and AFM can be attributed to the different timescales of molecular contact between BSA and the PNiPAM chains in the two experiments.

AFM data alone shown in Fig. 5 are not sufficiently accurate to shed light on the adhesion mechanism between the protein and the PNiPAM chains. More quantitative adsorption data as well as a more systematic analysis of this system will be required to elucidate this adhesion mechanism.

4. Summary and conclusion

We have synthesized a –SH terminated PNiPAM that responds to temperature changes in aqueous media, and prepared a thermally responsive monolayer (2.84 ± 0.2 nm) of this polymer on a gold surface. Surface analysis confirmed that the substrate was well covered with PNiPAM chains via Au–S bonds. Measurements of the water contact angle on the PNiPAM monolayer showed that the equilibrium and advancing contact angles at room temperature differ from those at 40 °C. An AFM study using a protein-immobilized tip showed that the intermolecular force between the PNiPAM monolayer and BSA is temperature dependent. Examination by QCA of the adsorption of BSA on the PNiPAM monolayer showed that the protein adsorption behavior varied with temperature. A discrepancy observed between the AFM and QCA results below the phase transition temperature was accounted for in terms of the different timescales of molecular contact between BSA and the PNiPAM monolayer in the two experiments. This finding suggests that AFM and QCA give different information on the adhesion between the protein and the PNiPAM chains.

Acknowledgements

This study was supported by a grant of the Korea Health 21 R and D project, Ministry of Health and Welfare, Korea. (02-PJ3-31402-0023).

References

- [1] Shibayama M, Tanaka T. *Advances in polymer science*, vol. 109. Berlin: Springer-Verlag; 1993. p. 1–62.
- [2] Tiktopulo EI, Bychkova VE, Ricka J, Ptitsyn OB. *Macromolecules* 1994;27:2879. Tiktopulo EI, Uversky VN, Lushchik VB, Klenin SI, Bychkova VE, Ptitsyn OB. *Macromolecules* 1995;28:7519.
- [3] Fujishige S, Kubota K, Ando I. *J Phys Chem* 1989;93:3311.
- [4] Zhu PW, Napper DH. *J Phys Chem B* 1997;101:3155. Zhu PW, Napper DH. *J Colloid Interf Sci* 1994;168:380.
- [5] Schild HG, Tirrell DA. *J Phys Chem* 1990;94:4352.
- [6] Matsuo ES, Tanaka T. *J Chem Phys* 1988;89:1695. Shibayama M, Shiwa Y, Rabin Y. *J Chem Phys* 1997;107:5227. Shibayama M, Suetoh Y, Nomura S. *Macromolecules* 1996;29:6966.
- [7] Takei YG, Aoki T, Sanui K, Ogata N, Sakurai Y, Okano T. *Macromolecules* 1994;27:6163. Yakushiji T, Sakai K, Kikuchi A, Aoyagi T, Sakurai Y, Okano T. *Langmuir* 1998;14:4657.
- [8] Liang L, Feng X, Peter JL, Rieke PC, Fryxell GE. *Macromolecules* 1998;31:7845.
- [9] Liang L, Rieke PC, Fryxell GE, Liu J, Engehard MH, Alford K. *J Phys Chem B* 2000;104:11667.
- [10] Schmitt F-J, Park C, Simon J, Ringsdorf H, Israelachvili J. *Langmuir* 1998;14:2838.
- [11] Balamurugan S, Mendez S, Balamurugan SS, O'Brien II MJ, Lopez GP. *Langmuir* 2003;19:2545.
- [12] Qui Y, Park K. *Adv Drug Deliv Rev* 2001;53:321.
- [13] Kaneko Y, Sakai K, Okano T. In: Okano T, editor. *Biorelated polymers and gels: controlled release and application in biomedical engineering USA*. Academic Press; 1998. p. 29–69. see also 93–134.
- [14] Okano T, Yamada N, Okuhara M, Sakai H, Sakurai Y. *Biomaterials* 1995;16:297. Recum H-V, Okano T, Kim SW. *J Controlled Release* 1998;55:121. Kwon OH, Kikuchi A, Yamato M, Sakurai Y, Okano T. *J Biomed Mater Res* 2000;50:82. Ebara M, Yamato M, Hirose M, Aoyagi T, Kikuchi A, Sakai K, Okano T. *Biomacromolecules* 2003;4: 344.
- [15] Stile RA, Burghardt WR, Healy KE. *Macromolecules* 1999;32:7370. Stile RA, Healy KE. *Biomacromolecules* 2001;2:185.
- [16] Fong RB, Ding Z, Long CJ, Hoffman AS, Stayton PS. *Bioconjugate Chem* 1999;10:720.
- [17] Garret-Flaudy F, Freitag R. *Biotech Bioeng* 2001;71:223.
- [18] Jones DM, Smith JR, Huck WTS, Alexander C. *Adv Mater* 2002;14: 1130.
- [19] Kanazawa H, Kashiwase Y, Yamamoto K, Matsushima Y, Kikuchi A, Sakurai Y, Okano T. *Anal Chem* 1997;69:823. Yakushiji T, Sakai K, Kikuchi A, Aoyagi T, Sakurai Y, Okano T. *Anal Chem*. 1999;71: 1125.
- [20] Ista LK, Mendez S, Perez-Luna VH, Lopez GP. *Langmuir* 2001;17: 2552.
- [21] Gan D, Lyon LA. *Macromolecules* 2002;35:9634.
- [22] Cunliffe D, Alarcon CH, Peters V, Smith JR, Alexander C. *Langmuir* 2003;19:2888.
- [23] Kidoaki S, Ohya S, Nakayama Y, Matsuda T. *Langmuir* 2001;17: 2402.
- [24] Pan YV, Wesley RA, Luginbuhl R, Denton DD, Ratner BD. *Biomacromolecules* 2001;2:32.
- [25] Shan J, Nuopponen M, Jiang H, Kauppinen E, Tenhu H. *Macromolecules* 2003;36:4526.

- [26] Niwa M, Matumoto T, Izumi H. *J Macromol Sci A* 1987;24:567. Niwa M, Sako Y, Shimizu M. *J Macromol Sci A* 1987;24:1315.
- [27] Niwa M, Shimoguchi M, Higashi N. *J Colloid Interf Sci* 1992;148:592.
- [28] Deakin MR, Butty DA. *Anal Chem* 1989;61:1147A.
- [29] Socrates G. *Infrared characteristic group frequencies*, 2nd ed. Great Britain: Wiley; 1994. p. 69.
- [30] Bandrup J, Immergut EH, Grulke EA, editors, 4th ed. *Polymer handbook*, vol. 2. Canada: Wiley; 1999. p. 47.
- [31] Moulder JF, Stickle WF, Sobol PE, Bomben KD. In: Chastain J, editor. *Handbook of X-ray photoelectron spectroscopy*. USA: Perkin-Elmer Corporation; 1992. p. 183.
- [32] Cho EC, Kim YD, Cho K. Submitted for publication.
- [33] Brown JR, Shockley P. In: Jost PC, Griffith OH, editors. *Lipid-protein interactions*, vol. 1. USA: Wiley; 1982. p. 25.
- [34] Petrash S, Sheller NB, Dando W, Foster MD. *Langmuir* 1997;13:1881. Sheller NB, Petrash S, Foster MD. *Langmuir* 1998;14:4535. Petrash S, Cregger T, Zhao B, Pokidysheva E, Foster MD, Brittan WJ, Sevastianov V, Majkrzak CF. *Langmuir* 2001;17:7645. Choi EJ, Foster MD. *Langmuir* 2002;18:557.
- [35] Otake K, Inomata H, Konno M, Saito S. *Macromolecules* 1990;23:283. Suetoh Y, Shibayama M. *Polymer* 2000;41:505. Grinberg VY, Dubovik AS, Kuznetsov DV, Grinberg NV, Grosberg AY, Tanaka T. *Macromolecules* 2000;33:8685. Feil H, Bae YH, Feijen J, Kim SW. *Macromolecules* 1993;26:2496. Cho EC, Lee J, Cho K. *Macromolecules* 2003;36:9929.
- [36] Tamai Y, Tanaka H, Nakanishi K. *Macromolecules* 1996;29:6750.
- [37] Mcpherson TB, Lee SJ, Park K. In: Horbett TA, Brash JL, editors. *Proteins at interfaces II*. Washington DC: American Chemical Society; 1995. p. 396.
- [38] Wang RLC, Kreuzer HJ, Grunze M. *J Phys Chem B* 1997;101:9767. Feldman K, Hahner G, Spencer ND, Harder P, Grunze M. *J Am Chem Soc* 1999;121:10134.
- [39] Jackson DR, Omanovic S, Roscoe SG. *Langmuir* 2000;16:5449. Sakiyama T, Toyomasu T, Nagata A, Imamura K, Nakanishi K, Takahashi T, Nagai T. *J Chem Engng Jpn* 1998;31:208.
- [40] Fujimoto K, Mizuhara Y, Tamura N, Kawaguchi H. *J Intelligent Mater Sys Struct* 1993;4:184.
- [41] Calonder C, Tie Y, Tassel PRV. *Proc Natl Acad Sci* 2001;98:10664. Sukhishvili SA, Dhinojwala A, Granick S. *Langmuir* 1999;15:8474. Wertz CF, Santore MM. *Langmuir* 1999;15:8884.